DRFC/CAD

Resumé fait

9900143?

EUR-CEA-FC-1656

High RF Power Test of a Lower Hybrid Module Mock-up in Carbon Fiber Composite

M. Goniche, P. Bibet, J. Brossaud, V. Cano,
P. Froissard, F. Kazarian, G. Rey,
S. Maebara, K. Kiyono , M. Seki,
K. Suganuma, Y. Ikeda, T. Imai

February 1999

ASSOCIATION EURATOM-C.E.A.
DEPARTEMENT DE RECHERCHES
SUR LA FUSION CONTROLEE
CEA/CADARACHE
13108 SAINT PAUL LEZ DURANCE CEDEX

Please be aware that all of the Missing Pages in this document were originally blank pages

High RF power test of a lower hybrid module mock-up in carbon fiber composite

M.Goniche, P.Bibet, J.Brossaud, V.Cano, P.Froissard, F.Kazarian-Vibert, G.Rey

Association Euratom-CEA
CEA/Cadarache
F-13108 Saint Paul-lez-Durance, France

S.Maebara[1], K.Kiyono[2], M.Seki[2], K. Suganuma[2], Y.Ikeda[2], T.Imai[1]

[1] Department of Fusion Engineering Research
[2] Department of Fusion Facility
Naka Fusion Research Establishment
Japan Atomic Energy Research Institute

Contents

Abstract

A mock-up module of a Lower Hybrid Current Drive antenna module of a Carbon Fiber Composite(CFC) was fabricated for the development of heat resistive front facing the plasma. This module is made from CFC plates and rods which are copper coated to reduce the RF losses. The withstand-voltage, the RF properties and outgassing rates for long pulses and high RF power were tested at the Lower Hybrid test bed facility of Cadarache.

After the short pulse conditioning, long pulses with a power density ranging between 50 and 150 MW / m^2 were performed with no breakdowns. During these tests, the module temperature was increasing from 100-200 °C to 400-500 °C. It was also checked that high power density, up to 150 MW/m^2, could be transmitted when the waveguides are filled with H_2 at a pressure of $5x10^{-2}$ Pa. No significant change in the reflection coefficient is measured after the long pulse operation. During a long pulse, the power reflection increases during the pulse typically from 0.8 % to 1.3 %. It is concluded that the outgassing rate of Cu-plated CFC is about 6 times larger than of Dispersion Strengthened Copper (DSC) module at the module temperature of 300 °C. No significant increase of the global outgassing of the CFC module was measured after hydrogen pre-filling. After the test, visual inspection revealed that peeling of the copper coating occurred at one end of the module only on a very small area ($0.2cm^2$).

It is assessed that a CFC module is an attractive candidate for the hardening of the tip of the LHCD antenna.

1. Introduction

In the frame of the collaboration between JAERI and CEA, two modules for a Lower Hybrid Antenna Modules have been previously tested. Test Module I was a 4-waveguide module made of Al_2O_3 Dispersion Strengthened Copper (DSC). A large data base of outgassing rate during high RF power injection was established [1]. Test Module II was composed of a Power Poloidal Divider (PPD) and a 3 x 6 waveguide Multijunction. RF properties at low and high power were studied in combination with an other poloidal divider (Mode converter or E/H plane multijunction). Outgassing properties of such a complex system was also documented [2].

For the next step machine, the mouth of the antenna facing the plasma is an important issue. In present day experiments the antenna waveguides are metallic. The metal is copper-coated stainless steel on JET and JT-60U, an alloy of copper and zirconium on Tore Supra, DSC on TdeV. Sputtering and erosion may lead to an undesirable contamination of the plasma with metallic impurities. The mouth of the Lower Hybrid antenna has to be hardened with a low Z material to reduce such impurities.

A possible solution is to fabricate the entire multijunction from a Carbon Fiber Composite (CFC). The inside surfaces of this multijunction has to be Cu- plated in order to reduce the RF losses. Because of the difference of thermal expansion coefficients between copper and CFC, the Cu-plating on CFC material is a key of fabrication technique. In order to establish this fabrication technique, heat resistivity test is first needed to check Cu adherance and bonding defect. Second, an RF test using long pulses at high power is needed for the RF properties, the withstand voltage and the outgassing rate.

For the first point, a 8GHz mock-up module using CFC was fabricated by JAERI, the heat resistivity test was done on JAERI Electron Beam Irradiation Stand (JEBIS) [3]. For irradiation heat fluxes up to 3.2 MW/m^2 for 2 min, no peeling of the Cu-plating and no bonding defects were observed. This heat load of 3.2 MW/m^2 is about 13 times higher than the steady-state average heat load on the first wall of ITER.

The second point is the main part of this report. Test module III is a CFC module fabricated with the same technique as used for the 8GHz mock-up module. In order to compare the RF properties, withstand-voltage and outgassing rates, a reference module in DSC was also fabricated. These two components were fabricated by JAERI and tested at the lower hybrid test bed facility of Cadarache in the frame of the collaboration. The CFC and DSC modules are described in section 2. The experimental set-up for high power test is presented in section 3. The low power measurements are given in section 4 whereas RF properties at high power are presented in section 5. The different outgassing measurements are discussed in section 6. Details on module inspection after test are given in section 6. Finally conclusions are drawn.

2. The Module III

Table 1 shows the main physical properties of CFC and DSC. The melting point of CFC material is about 3 times higher than that of DSC. However, electric resistivity of CFC material is about 70 times higher than DSC. The high resistivity is favorable from the point of the electro-magnetic force in case of plasma disruption but it makes large ohmic losses in the waveguides. The Cu-plating is therefore indispensable on the inside surfaces of the CFC waveguide. Because of the difference of thermal expansion coefficients between copper and CFC, by almost a factor of 3, a compliant layer is needed and the Cu-plating is

advantageously used as the interface layer for assembling the septum plates to rods and the cooling channel to the CFC module.

	Unit	CFC	Cu-Al2O3
Melting point	°C	3923	1356
Density ρ	$kg.m^{-3}$	1880	8860
Resistivity (400°C)	10^{-8} Ω.m	350	4.9
Specific heat c_p (400°C)	$J.kg^{-1}.K^{-1}$	1450	413
Coefficient of thermal expansion (400°C)	10^{-6} K^{-1}	6.3	17.1
Thermal conductivity k (400°C)	$W.m^{-1}.K^{-1}$	320	300

Table 1. Main physical properties of CFC and DSC.

The CFC is a two-dimensional structure (Toshiba Corporation). This CFC is knitted with an intersecting angle of 15° to increase bending strength of the septum plate. The carbon fiber diameter is 10 μm and the bundle number is 3000. The fabrication flow chart for the mock-up module using CFC material is shown in Fig. 1. First, four septum plates and six rods were accurately cut from CFC material and the cleaning of pieces was done by ultrasonic waves. Second, each pieces were coated with titanium by physical vapor deposition. The thickness of Ti layer is 5 ~ 8 μm. Third, copper was electrochemically plated on top of the Ti layer, a copper plating of 20~30 μm was deposited by electrochemical deposition. After outgassing treatment of these pieces, septum plates and rods were assembled by diffusion bonding method at a temperature of 920 °C and an isostatic pressure of ~ 20 MPa. Finally, the copper cooling channels were silver brazed on the module at 820 °C. In these process, the CFC outgassing treatment is a crucial step. An incomplete treatment would lead to a loss of adherence of the copper when diffusion bonding or silver brazing is carried out.

Two test modules were fabricated by JAERI. These modules are only different by the material used for fabrication. The first one is made from DSC plates and rods and is used as a reference and the second is made from CFC copper-plated plates and rods. The DSC module is assembled by silver brazing. The CFC module is assembled and copper plated with the same techniques than for the 8GHz module mock-up.

The photograph- of the 3.7 GHz module is shown in Fig. 2. The length is 206 mm and the inner dimension of the secondary waveguides is 19 x 72 mm. At each end, a choke flange is used as shown in Fig.3. The choke length is 49.95 mm (~ λg / 2), the nominal gap length is 3 mm.

3. The experimental set-up

The experimental set-up is sketched in Fig. 4. The total under vacuum length is 1.2 m. Each window is connected to a bellow for the vacuum tightness. Inside the bellow, a standard waveguide is in contact with the window. Between the waveguide and the test module, a taper waveguide (from 36 x 76 to 34 x 72 mm) is connected. This taper waveguide (L=200 mm),

made from brazed copper-coated plates, is vacuum tight. Because of the low conductance between the inside and the outside of the module, two pumping pipes were connected. Pumping of the inside was provided by a low conductance ϕ12 mm port and pumping of the outside was provided by a ϕ114 mm port. Taking into account the connection pipes between the ports and the turbo-molecular pump, the total effective pumping speed is estimated to be only 0.01 m^3/sec. A ion gauge allows to measure the pressure outside of the module. Three thermocouples were connected to the module. These under vacuum thermocouples allow to control the temperature of the module at different locations of the same transverse section. One thermocouple was installed on each taper waveguide.

The DSC reference module was tested first. The module was baked at 300 °C for 50 h. After cooling, an air leak was detected and the system had to be vented in order to repair the leak. Then the module was baked at 300 °C for 16 h. For the CFC module, only a 300°C/16h baking was achieved.

4. Low power measurements

Low power measurements were performed before and after the high power test. The S_{21} and S_{11} parameters were measured from the input RF window to the output window in the 3.6-3.8 GHz band. In the entire frequency range, S_{21} is below 0.1 dB for both modules, indicating a transmission factor higher than 0.98. The calculation of the RF losses of the 1.2 m long waveguides leads to a transmission factor of 0.994 at room temperature.
S_{11} is larger than 20 dB in the frequency range. The different values at 3.70 and 3.73 GHz are listed in table 2. For the CFC module, no significant change of S_{11} is measured.

S_{11} (dB)	DSC module		CFC module	
	3.70 GHz	3.73 GHz	3.70 GHz	3.73 GHz
Before experiment	-26.8	-28.4	-25.5	-21.7
After experiment	-28.8	-23.0	-24.9	-21.6

Table 2. S_{11} parameter of the 2 modules

5. RF properties at high power

5.1 RF conditioning

The same RF conditioning technique for the module I and II was used. First, the RF power was gradually increased using 10 msec every 100 ms. For the DSC module, the first breakdown occurred at 110 kW (48 MW/m^2 - E_{rf}= 3.0 kV/cm), and the 150 MW / m^2 - E_{rf}= 5.3 kV/cm), level was obtained after 30,000 pulses. For the CFC module, the first breakdown was detected almost at the same power (100 kW) but the conditioning was faster. Only 10,000 pulses were needed to reach the 150 MW / m^2 level (Fig.5). This may indicate that conditioning of the connections waveguides or / and RF windows which were baked at a lower temperature than the module was the most demanding in terms of number of pulses.

After this short pulse conditioning, two second pulses at the 100 MW/m^2 level were easily achieved with no breakdowns and long pulse operation was started. After long pulse operation at the 100 MW / m^2 level, conditioning at higher power was achieved and a record power of 390 kW (170 MW / m^2) was obtained for 6 sec (Fig.6). For each module, 12 long pulses with a power density ranging between 50 and 140 MW / m^2 were performed. During these long pulses, the module temperature was increasing between 100-200 °C and 400-500 °C (Fig.7). A typical shot at 90 MW / m^2 is shown in Fig.8. All these tests were performed with an initial pressure of ~ 10^{-4} Pa. It was checked that high power density, at least up to 150 MW / m^2, could be transmitted when the waveguides are filled with H_2 at a pressure of $5x10^{-2}$ Pa.

5.2 Power reflection coefficient

The power reflection coefficient (RC) was calculated from the RF measurements available at the output of the klystron, ~ 0.5 m upstream the input RF window. For an input power of 120 kW, this reflection coefficient is quoted at the beginning of the high power test and after all the long pulse operation for the 2 modules. The results are given in table 3.

RC. (%)	DSC module	CFC module
before experiment	0.55 % (T=50°C)	0.90 % (T=45°C)
after experiment	0.90% (T=175°C)	0.82 % (T=55°C)

Table 3 Reflection coefficients of the 2 modules

Low reflection is measured for the 2 modules (<1 %). No significant modification of the RC is measured after the long pulse operation. During a long pulse, the reflection increases during the pulse typically from 0.4 % to 0.9 % (Fig.8). The same behavior was observed in previous long pulse RF tests. The main reason is the change of phase of the reflected wave due to thermal expansion which has to be taken into account for a directional coupler with a finite directivity. With the following parameters :

L = 1.2 m
a = $1.7\ 10^{-5}\ K^{-1}$
RC. = 0.9 %
D = -30 dB

It is found that the measured reflected power increases by ~ 10 % for ΔT = 100 °C. Experimentally, it is found ~ 20 % for ΔT = 100 °C. The change of directivity of the coupler with the temperature may also influence the measurement of the reflected power.

5.3 RF losses

RF losses were estimated from the temperature increase rate measured on the thermocouples attached to the module. At f = 3.7 GHz, the RF losses P (in W/m^2) of a waveguide of height a and width b are given by :

$$P_a = \frac{0.3206\sqrt{\rho_{el}}\left[1-(1-\frac{\lambda_0^2}{2a^2})\cos\frac{2\pi x}{a}\right]}{\sqrt{1-\frac{\lambda_0^2}{4a^2}}}P \qquad (1)$$

along the large side a of the waveguide.

$$P_b = \frac{0.3206\sqrt{\rho_{el}}\left[\frac{\lambda_0^2}{2a^2}\right]}{\sqrt{1-\frac{\lambda_0^2}{4a^2}}}P \qquad (2)$$

along the small side b of the waveguide, where ρ_{el} is the resitivity (in Ω.m), P the RF power density (in W/m^2) and λ_0 the wavelength in vacuum (0.081m). P_a is maximum for x=a/2 (mid-height) and is equal to

$$P_a^{max} = \frac{0.3206\sqrt{\rho_{el}}\left[2-\frac{\lambda_0^2}{2a^2}\right]}{\sqrt{1-\frac{\lambda_0^2}{4a^2}}}P \qquad (3)$$

the average losses per unit of length <P> (in W/m) are given by

$$\langle P\rangle = \frac{0.3206\sqrt{\rho_{el}}\left[2a+2b\frac{\lambda_0^2}{2a^2}\right]}{\sqrt{1-\frac{\lambda_0^2}{4a^2}}}P \qquad \text{(1 waveguide) (4)}$$

For the module III, with a =0.072 m and b = 0.019 m, the losses as a function of the temperature are given in table 4 for P = 100MW/m^2.

T (°C)	50	150	250	350

ρ_{el} (10^{-8} Ω.m)	2.0	2.8	3.7	4.6
P_a^{max} (W/m^2)	7495	8870	10195	11365
P_b (W/m^2)	3480	4120	4735	5280
<P> (W/m) (for the 2 waveguides)	1845	2185	2510	2800

Table 4. Calculated RF losses for module III

The local heating rate is given by

$$\frac{dT}{dt} = \frac{P_{a\,or\,b}}{\rho e c_p} \qquad (5)$$

where e (in m) is the thickness of the walls

ρ (in kg m^{-3}) is the volume density of the material

c_p (in J kg^{-1} K^{-1})

The average heating rate is given by

$$\frac{dT}{dt} = \frac{<P>}{\rho S c_p} \qquad (6)$$

where S is the section surface of the module (S=8.80x10^{-4} m^2). For the DSC module the heating rates corresponding to P_a^{max} (T_1) or to P_b (T_2 and T_3) are given in Table 5 for P = 100 MW / m^2.

T (°C)	50	150	250	350
P_a^{max}(W/m^2)	7495	8870	10195	11365
$\rho e c_p$ (Jm^{-2}K^{-1}) (e=0.2 cm, ρ=8.86 g.cm^{-3} c_p=0.39-0.41J g^{-1}K^{-1})	6911	7088	7212	7301
dT_1/dt (K/s)	1.08	1.25	1.41	1.56
P_b (W/m^2)	3480	4120	4735	5280
$\rho e c_p$ (Jm^{-2}K^{-1}) (e=0.7cm, ρ=8.86 g.cm^{-3} cp=0.39-0.41Jg^{-1}K^{-1})	24188	24808	25242	25553
$dT_{2/3}/dt$ (K/s)	0.14	0.17	0.19	0.21
<P> (W/m) (for the 2 waveguides)	1845	2185	2510	2800
$\rho S c_p$ (Jm^{-2}K^{-1}) (S=8.8cm^2, ρ=8.86g.cm^{-3} c_p=0.39-0.41Jg^{-1}K^{-1})	3041	3119	3174	3213
dT/dt (K/s) ($t>>\tau$)	0.61	0.70	0.79	0.87

Table 5. Heating rates for the DSC module at P=100 MW/m^2

For the CFC module, the heating rates at 100 MW / m^2 are given in table 6.

P_a^{max} (W/m^2)	7495	8870	10195	11365
ρec_p ($J.m^{-2}K^{-1}$) (e=0.2 cm, ρ=1.79 gcm^{-3} c_p=0.76-1.39 $Jg^{-1}K^{-1}$)	2735	3755	4464	4976
dT_1/dt (K/s)	2.74	2.36	2.28	2.28
P_b (W/m^2)	3480	4120	4735	5280
ρec_p($J.m^{-2}K^{-1}$) (e=0.7cm, ρ=8.86 $g.cm^{-3}$ c_p=0.76-1.39 $Jg^{-1}K^{-1}$)	9572	13142	15624	17416
$dT_{2/3}/dt$ (K/s)	0.36	0.31	0.30	0.30
<P> (W/m) (for the 2 waveguides)	1845	2185	2510	2800
ρSc_p($J.m^{-2}K^{-1}$) (S=8.8cm^2, ρ=1.79$g.cm^{-3}$ c_p=0.76-1.39 $Jg^{-1}K^{-1}$)	1203	1652	1964	2189
dT/dt (K/s) ($t>>\tau$)	1.53	1.32	1.28	1.28

Table 6 Heating rates for the CFC module at 100 MW/m^2

In fact with heat diffusion, the thermocouple will indicate a heating rate given by Eq.6 after a time much larger than the time constant $t = L^2/D$ where $L = a/2 = 0.036$ m and $D(=k/\rho c_p)$ the diffusivity of the material. τ for the DSC and the CFC are given in table 7.

	DSC	CFC
$D(m^2/s)$	1.03×10^{-4} at 20 °C 0.87×10^{-4} at 300 °C	2.23×10^{-4} at 20 °C 0.76×10^{-4} at 300 °C
τ (s)	12.6 s at 20 °C 14.9 s at at 300 °C	5.8 s at 20 °C 17.0 s at 300 °C

Table 7. Diffusivity and time constant for DSC and CFC

For the DSC module, as expected, the thermocouple (T_1) located at mid-height of the module has a much higher rate than the one attached to the small side of the waveguide (T_2). For different power densities, the experimental and the calculated rates are compared for T_1 and T_2. For T_1, the experimental value, measured on ~ 10 s is lower than the one given by the calculation (~ -15%), whereas the experimental value is higher for T_2 (Fig.9). This can be consistent, if we consider that diffusion, from $x = a/2$ to $x = a$, is not negligible on a time scale $t=10$ s ($t \sim \tau$).

After ~100 s, the heating rate is the same for the 3 thermocouples. The experimental and calculated heating rates are compared for three RF power densities. Experimental values are systematically lower than the calculated ones. This is not surprising if we consider diffusion, now along the RF propagation is effective on a time scale of 100 s (Fig.10).

For the CFC module, it was found anomalous time evaluations of temperature given by the 3 thermocouples attached to the module. Moreover, one of the TC blew off during the

second long pulse. This anomalous behavior is due to direct heating of the TC by RF leaking from the input choke flange. This leak is likely to occur from time to time and an attempt to compare the experimental and calculated heating rates were nevertheless performed.

The initial heating rates, for 2 power densities, are indicated on Fig.11. The heating rate at 100 MW / m^2, which is lower than predicted, is consistent with measurements made on the DSC module. After heat diffusion, at $t \sim 100$ s ($t >> \tau$), the experimental and calculated heating rates are compared on Fig.12. For this case, when comparing to the results of the DSC module, slightly lower heating rates should be measured.

6. Outgassing measurements

6.1 Outgassing measurement of CFC samples

Outgassing measurements of samples in CFC, CFC with Cu-plating and DSC were carried out at JAERI. The dimension of the test pieces is 100 x 20 x 5 mm^3. Two pieces were installed to increase surface area. The total outgassing surface area of the test pieces is 0.01 m^2. The test pieces and the experimental set-up are shown in Fig.13. Pressure is measured on both sides of a low conductance(C=1 l/s) orifice. The outgassing flux Q is obtained from the pressure difference ($Q=C \times \Delta P$) when the left-hand side gate valve is closed (conductance method). Figure 14 indicates the outgassing flux at 300 °C as a function of the baking treatment time. It is deduced that the outgassing rate of Cu-plated CFC and CFC are almost the same after ~ 80 hours of baking($\sim 10^{-5}$ Pam^{-3} $s^{-1}m^{-2}$). It is also inferred that the outgassing of CFC-based material is about one order of magnitude higher than that of DSC, after ~ 60 hours of 300 °C baking.

6.2 Outgassing measurements of module III

For the 15 long pulses performed on each module at high RF power, the outgassing flux was measured before and during RF injection at different times by the build-up method. For these pulses, the outgassing flux is plotted versus the module temperature in Fig. 15.

For the two modules, the initial outgassing before RF injection is, averaged on the different shots, the same : 2×10^{-7} $Pam^{-3}s^{-1}$ at 100 °C and $6\text{-}7 \times 10^{-7}$ $Pam^{-3}s^{-1}$ at 200 °C. During RF operation, the average outgassing flux is significantly higher for the CFC module by a factor ~2 at 200 °C and a factor ~4 at 350 °C. The outgassing rates were evaluated in both cases by taking into account the actual outgassing surface. In the case of DSC module, the 2 tapered waveguides and the 2 connection waveguides are almost at the same temperature as the module as shown in Fig.16. The total surface of these 5 components were considered (S=0.27 m^2). In the case of CFC module, because of the lower ρc_p value for CFC, the module heating rate is about 2 times the heating rates of the other waveguides(Fig.17), and only the surface of CFC module is considered (S=0.12 m^2). With such assumptions, the outgassing rate versus the module temperature is plotted in Fig.18. When comparing the data base from the two modules, it is concluded that the outgassing rate of Cu-plated CFC is 8 times larger than of DSC at the module temperature of 300-350 °C.

The effect of H_2 prefilling on the outgassing rate was investigated. After prefilling at $5x10^{-4}$ Pa for ~ 60s, the waveguides were pumped out for ~ 60 s. The pressure did not fully recover and the initial outgassing flux after H_2 pre-filling was about 2-3.5 times the outgassing flux before H_2 pre-filling. Due to this higher initial outgassing rate, the outgassing rate of CFC module, during RF operation, was about 2-3 times larger than the one of the DSC module.

7. Module inspection and surface analysis

After experiments, the two modules were inspected. Both modules show a good general aspect. No brazing defects were reported. This is consistent with the RF measurements which were made before and after the long pulse operation(see table 3 and 4). However on the CFC module peeling of the copper coating occurred on a very localized zone(S=0.8x0.2-0.3 cm^2), located at one end of the module. In the vicinity of this zone, traces of arcing were also observed. Arcing is believed to be due to the smaller gap length of the choke flange. The gap was measured for the two flanges of two modules. For the DSC module this gap varies between 2.5 and 2.9 mm, but on the DSC the variation is larger, between 2.1 and 3.1 mm and the minimum is effectively measured where the arcs occurred.

Black points were observed in the corners of the waveguides before the rf test. These black points were analyzed by X-ray diffraction technique. Only copper is seen and the change of colour is assumed to be due to an oxidation of the surface.

8. Conclusions

A 2-waveguide, 206 mm long, module in Carbon Fiber Composite (CFC) was tested first at low RF power, then in vacuum at high RF power (up to 150 MW/m^2). Good RF properties in the 3.67-3.73 GHz band was measured (VSWR >21 dB) with no resonance. The accuracy of the transmission factor measurement (±0.1 dB) allows only to assess that the rf losses are, at the most, 2% (expected value 0.6 %).

At high power (50-150 MW/m^2), RF losses were evaluated from thermocouples measurements during very long pulses (up to 2500 s). When compared to a reference module in a copper alloy (Dispersed Strengthened Copper), the RF losses seem slightly higher for the CFC module (~20%). However, because of an RF leak at one end of the module, the measurements on the CFC module has a poor accuracy and this results has to be confirmed.

The outgassing rate was measured for the CFC module and the DSC reference module. Neglecting the outgassing of the vacuum vessel for the both cases and the outgassing of the connection waveguides when connected to the CFC module, it is found that, despite the same initial outgassing, the outgassing rate is about 8 times higher at 350 °C for the CFC module than for the DSC module. However, such assumption lead to an over evaluation of the outgassing rate of CFC. Taking into account the outgassing of these waveguides, the outgassing rate of CFC is evaluated to 6~7 times the outgassing rate of DSC. Despite the same initial outgassing rate, the highest outgasing rate of CFC at high temperature might be due to a different composition of the desorbed gas for the 2 materials. It is deduced that the outgassing rate for the CFC module is about $4x10^{-5}$ $Pam^3s^{-1}m^{-2}$ at 300 °C and $3x10^{-4}$ $Pam^3s^{-1}m^{-2}$ at 400 °C. For the DSC module the average value of $5x10^{-5}$ $Pam^3s^{-1}m^{-2}$ at 400 °C is

comparable with the early measurements made on module I [1]. The effects of hydrogen prefilling was studied. When H_2 prefilling is performed, the outgassing during RF injection increases accordingly to the increase of the initial outgassing (factor 2-3.5). These results are rather consistent with previous results [1] and it is concluded that for module IV, first a longer baking time is required (60 hours instead of 15 hours at 300 °C), second a mass spectrometer is needed to monitor separately the outgassing of the hydrogen and the other species.

Visual inspection as RF measurements before and after long pulse operation indicate no degradation of the thin copper plating. However arcing and a very localized copper peeling ($S \sim 0.2$ cm^2) occurred at one end. This may be avoided by the appropriate design of the choke gap.

We assessed that CFC module is a promising material for the multijunction module of an LHCD antenna. More reliable data are needed to evaluate accurately the RF losses and the outgassing has to further studied.

Acknowledgments

The authors would like to express their thanks to all members of the RF facility division and RF heating laboratory at JAERI, and the LHRF group and secretaries at CEA-Cadrache for their continuous support. They would also like to acknowledge Drs. M.Chatelier, T.Nagashima, M.Ohta, S.Shimamoto, G.Tonon, J.G.Wegrowe and M.Yoshikawa for their encouragement of our collaborative activities.

References

[1] M. Goniche et al, Very long pulse high RF power test of a lower hybrid frequency antenna module, Rep. EUR-CEA-FC-1511, M. Seki et al., Performance test of a lower hybrid waveguide under long/high r.f. power transmission, JAERI-Research 96-025.
[2] S. Maebara et al., Development of a new lower hybrid antenna module using a poloidal power divider, JAERI-Research 96-036, Rep. EUR-CEA-FC-1590.
[3] S. Maebara et al., Development of plasma facing component for LHCD antenna, 4th Int. Symp. on Fusion Nuclear Technology, April 6-11,1997, Tokyo, Japan. Papers of the ISFNT-4 will be published in a special issue of Journal of Fusion Engineering and Design.

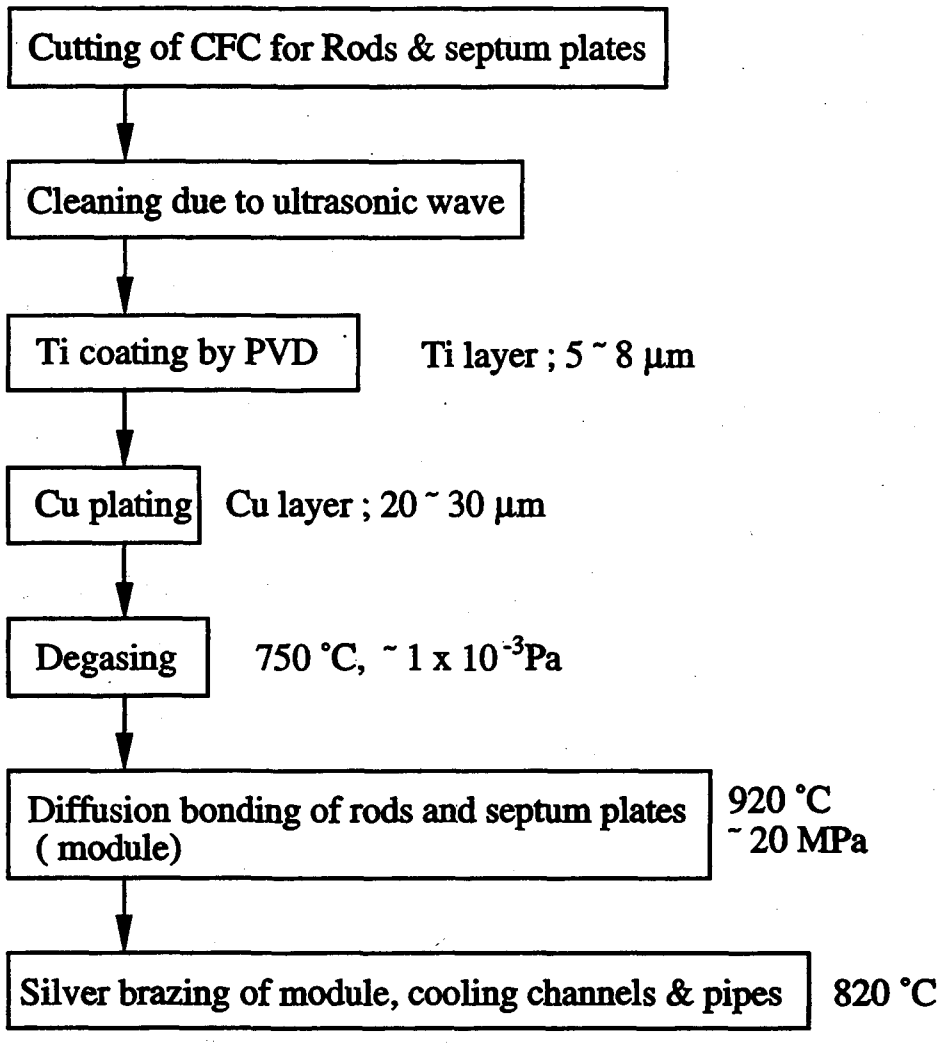

Fig. 1 Fabrication flow chart for the mock-up module using CFC material.

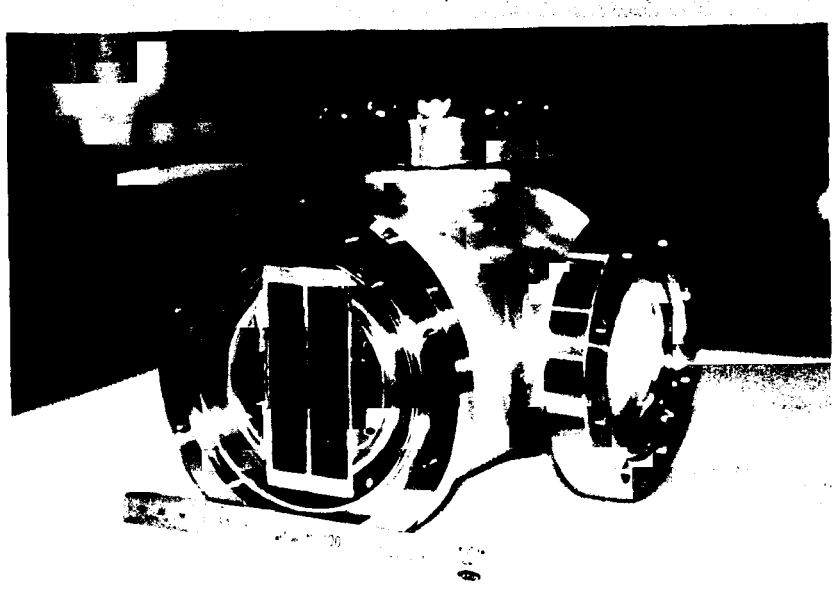

Fig.2 Photograph of 3.7 GHz CFC module.

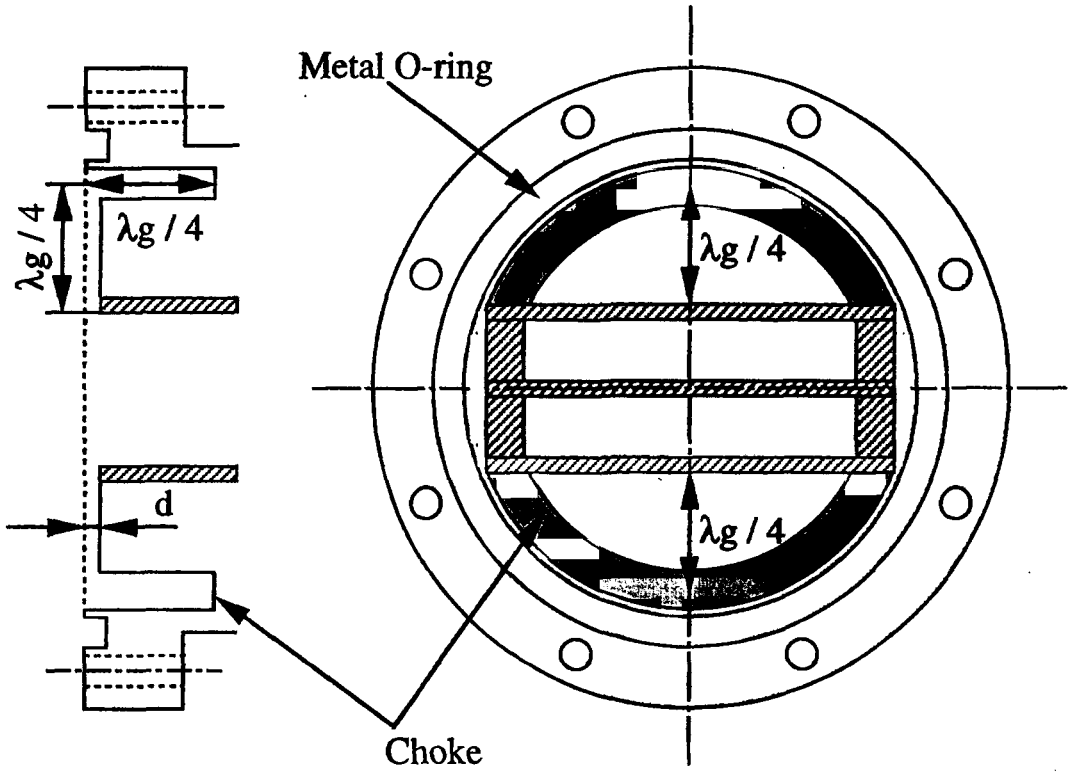

Fig.3 Cross section of the choke flange.

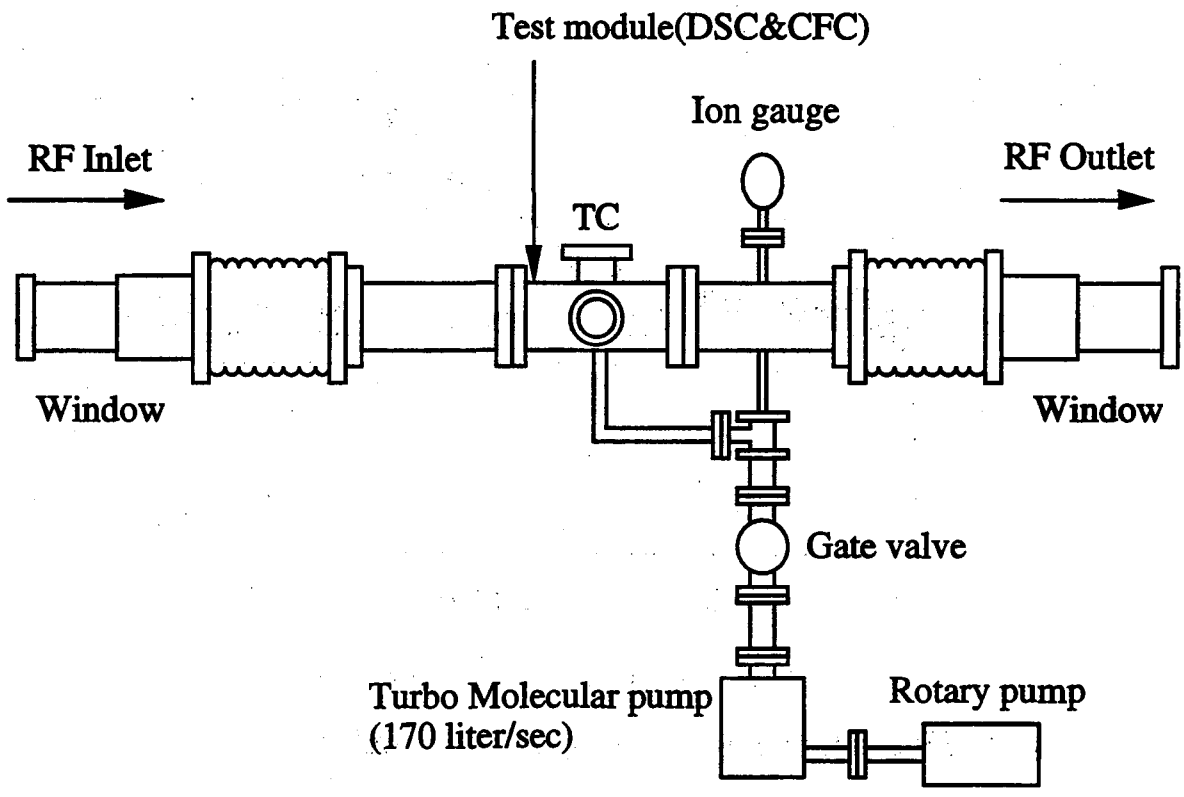

Fig. 4 Experimental Set-up.

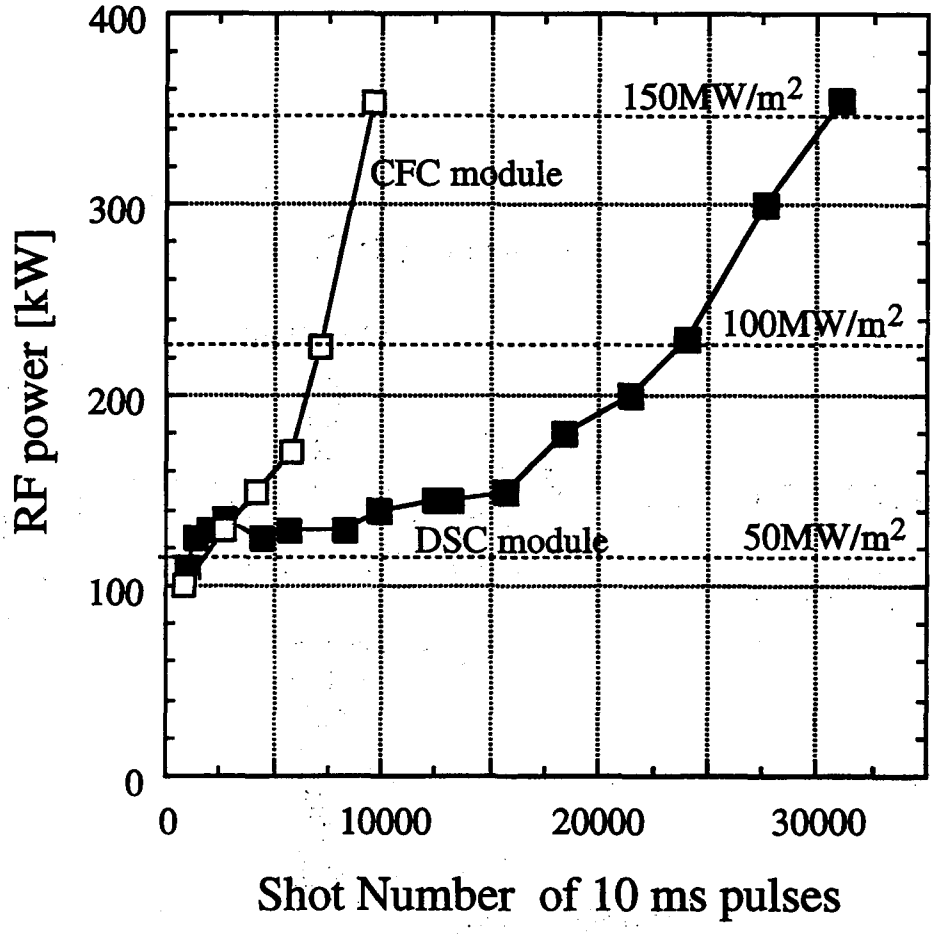

Fig. 5 RF conditioning of DSC and CFC modules

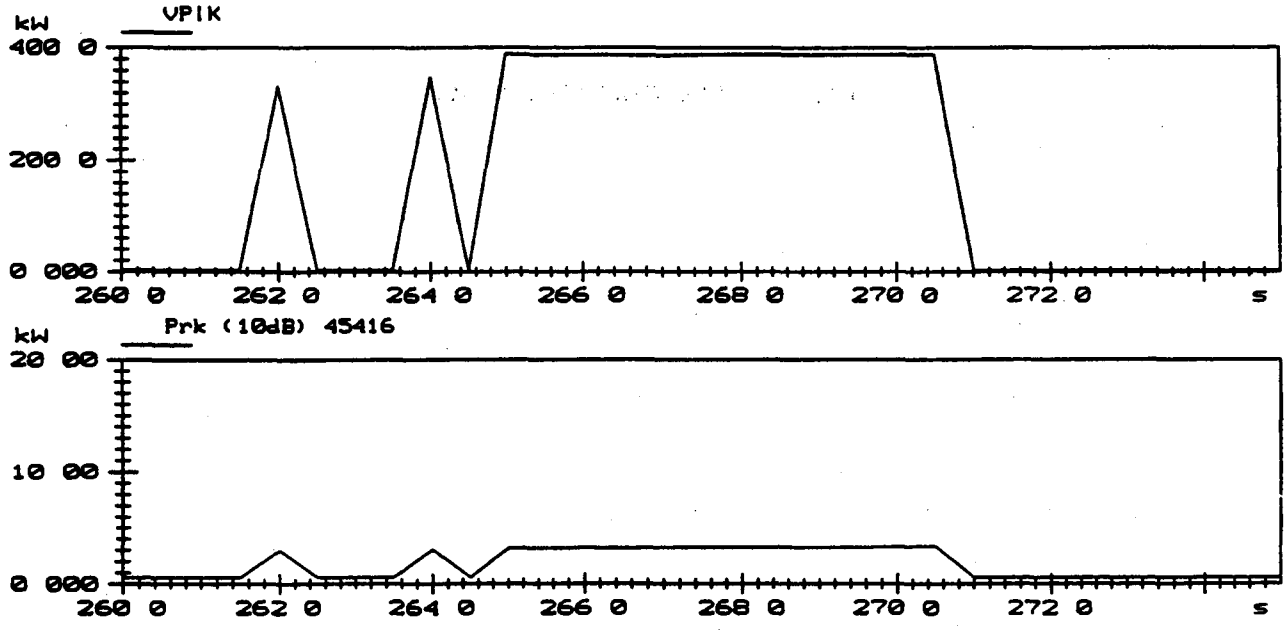

Fig. 6 High power test of the CFC module (170MW/m^2-6s)

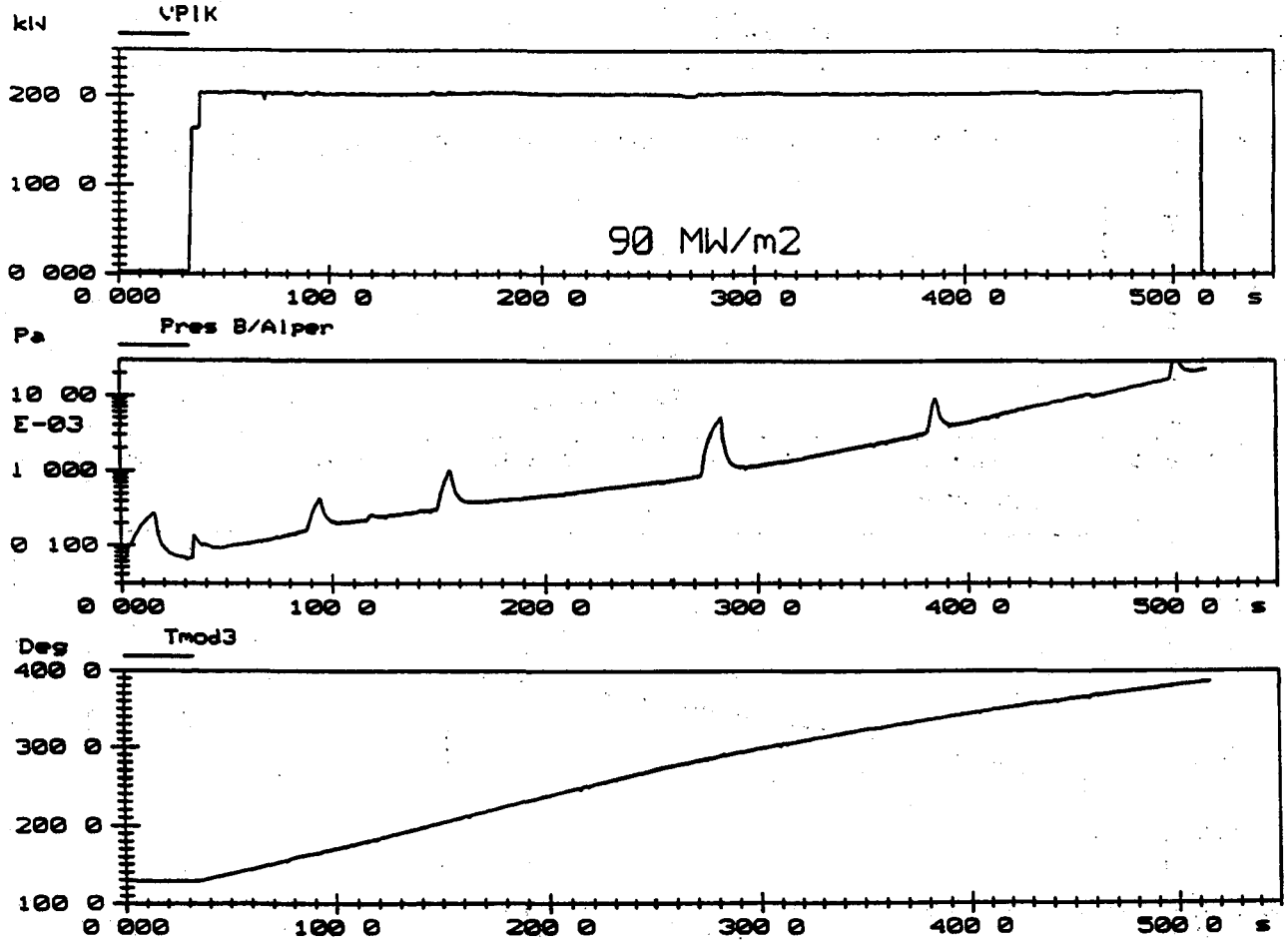

Fig.7 High power test of the CFC module (90MW/m^2-480s)
a) Incident power
b) Pressure
c) Temperature of the CFC module

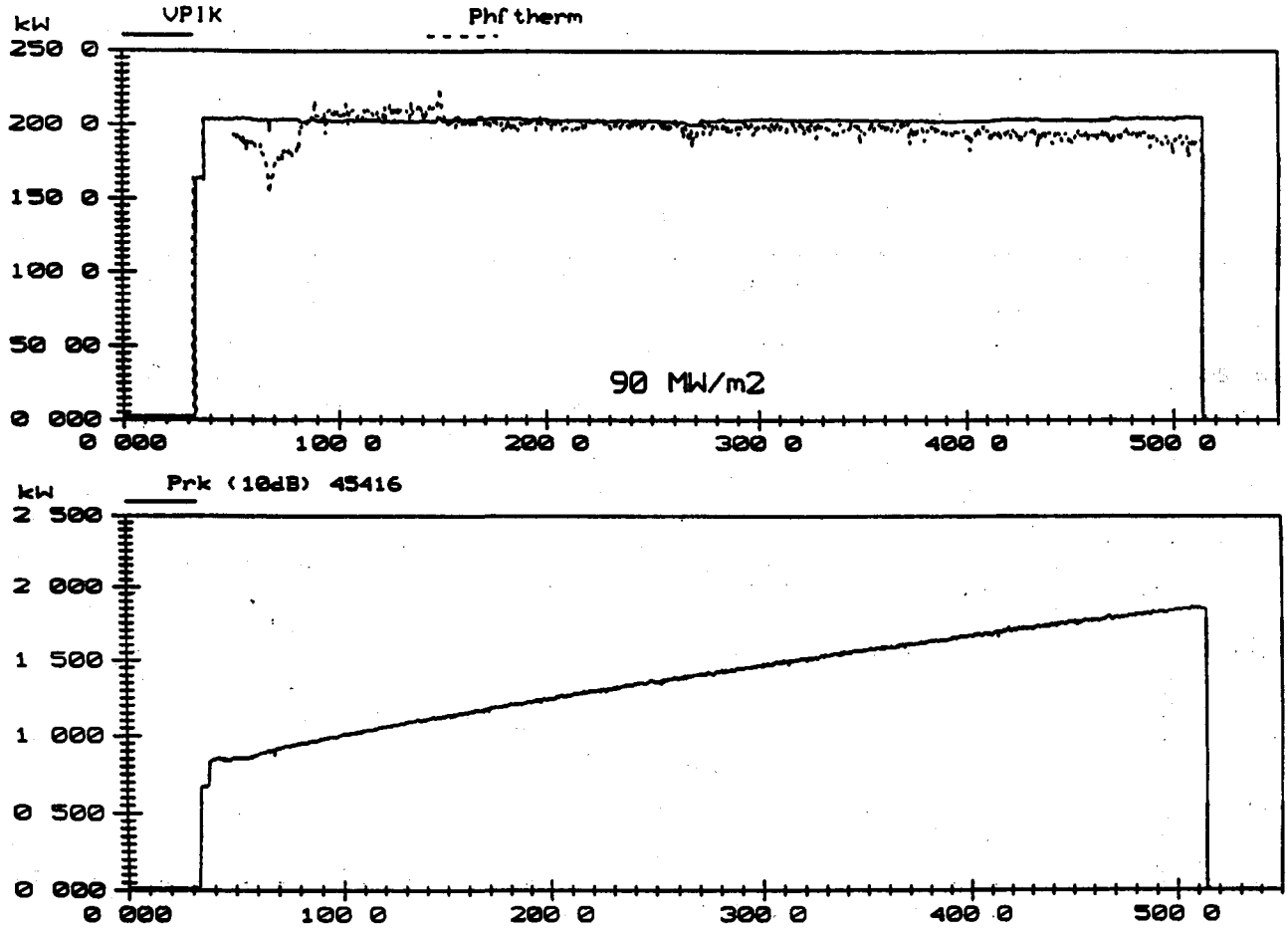

Fig.8 High power test of the CFC module (90MW/m^2-480s)

a) Incident power and calorimetric measurement of the power dumped in the end

b) Reflected power

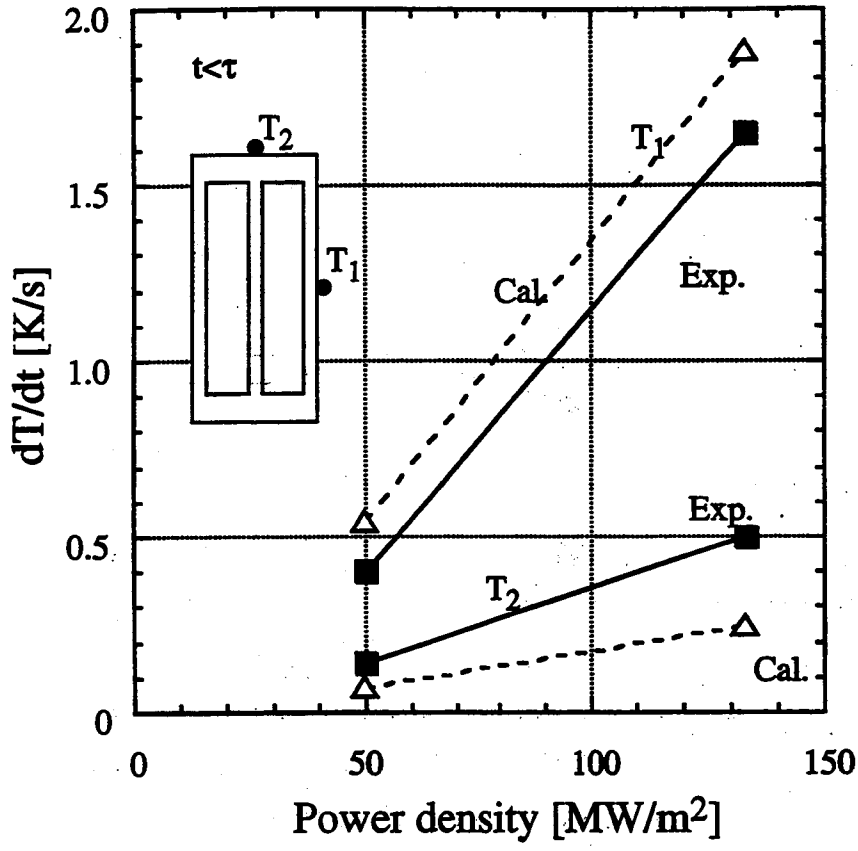

Fig.9 Calculated and experimental heating rates for the DSC module(t< τ).

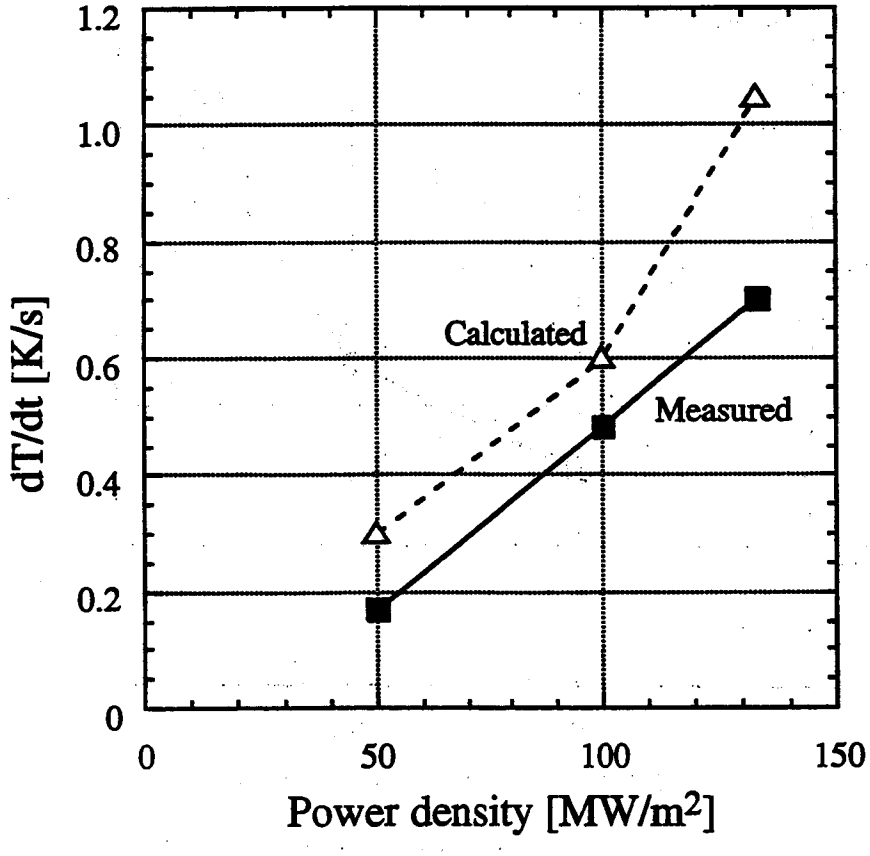

Fig.10 Calculated and experimental heating rates for the DSC module(t>> τ).

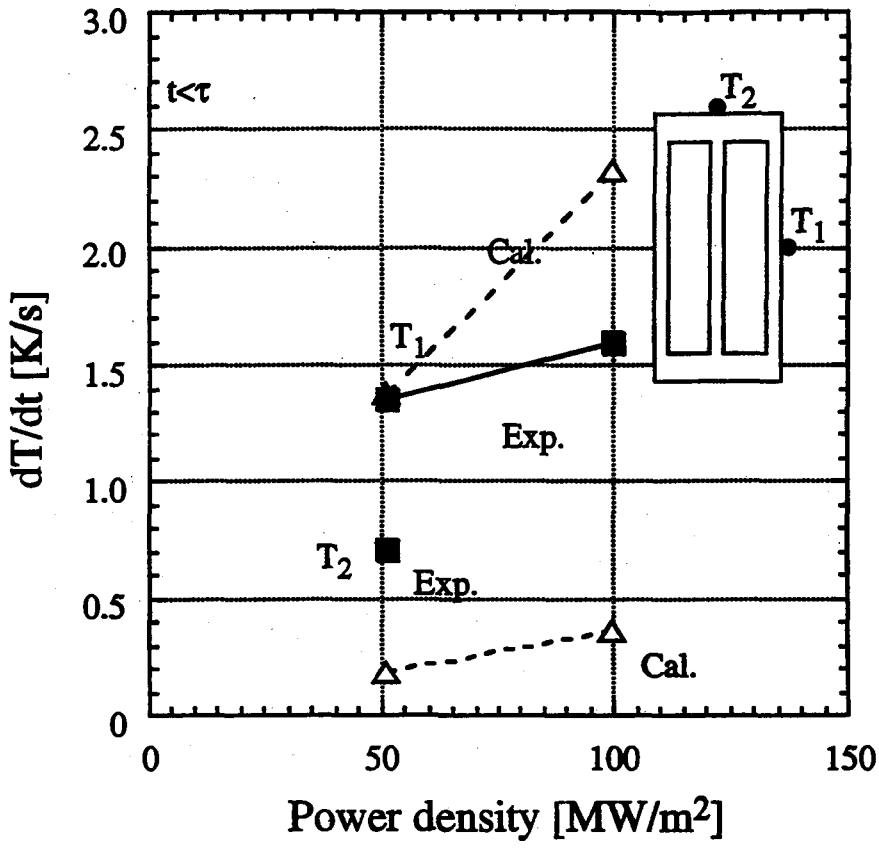

Fig.11 Calculated and experimental heating rates for the CFC module(t< τ).

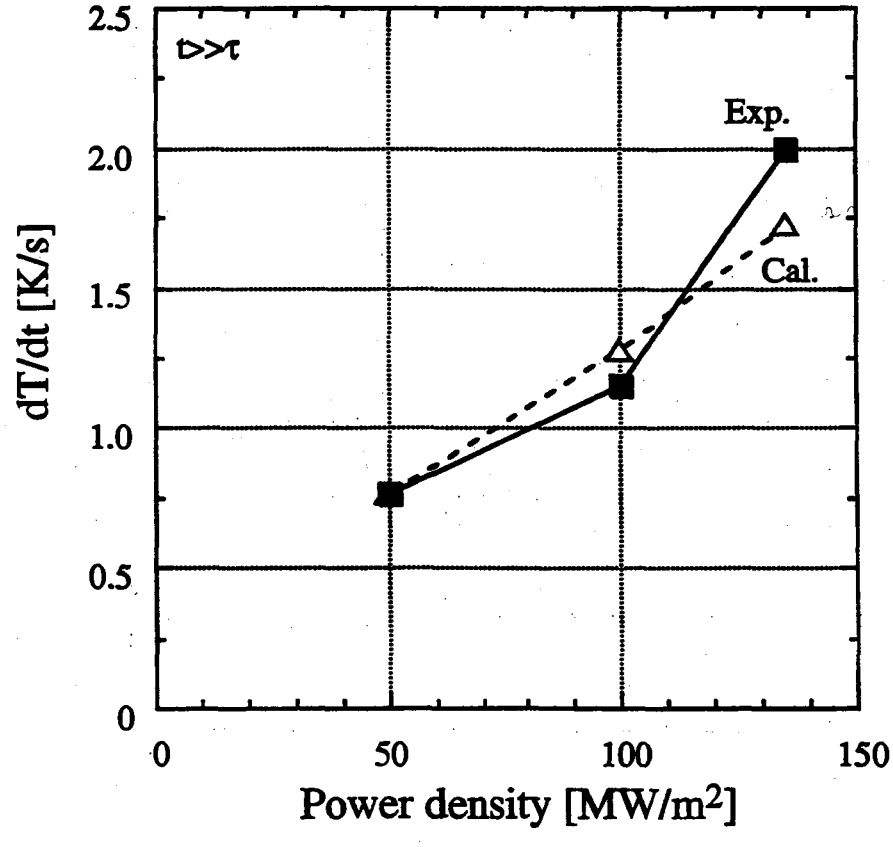

Fig.12 Calculated and experimental heating rates for the CFC module(t>> τ).

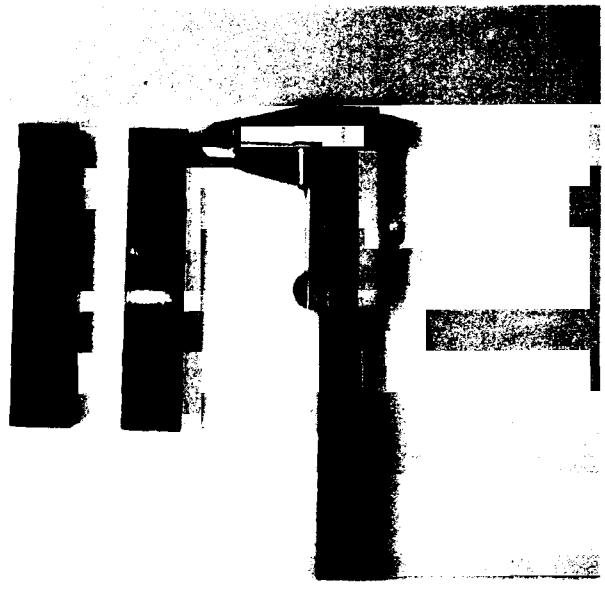

The test pieces of CFC and CFC with Cu plating

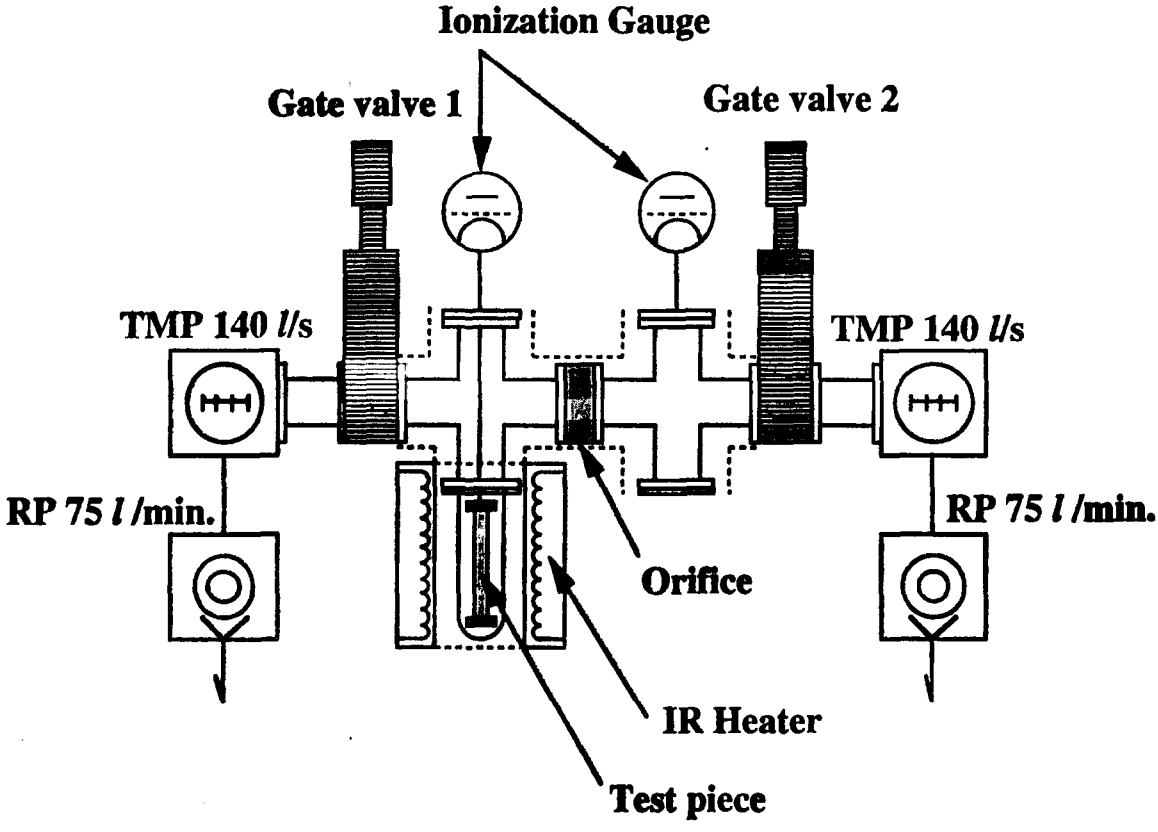

Fig.13 The experimental set-up for outgassing measurement of CFC, CFC with Cu plating and DSC test pieces.

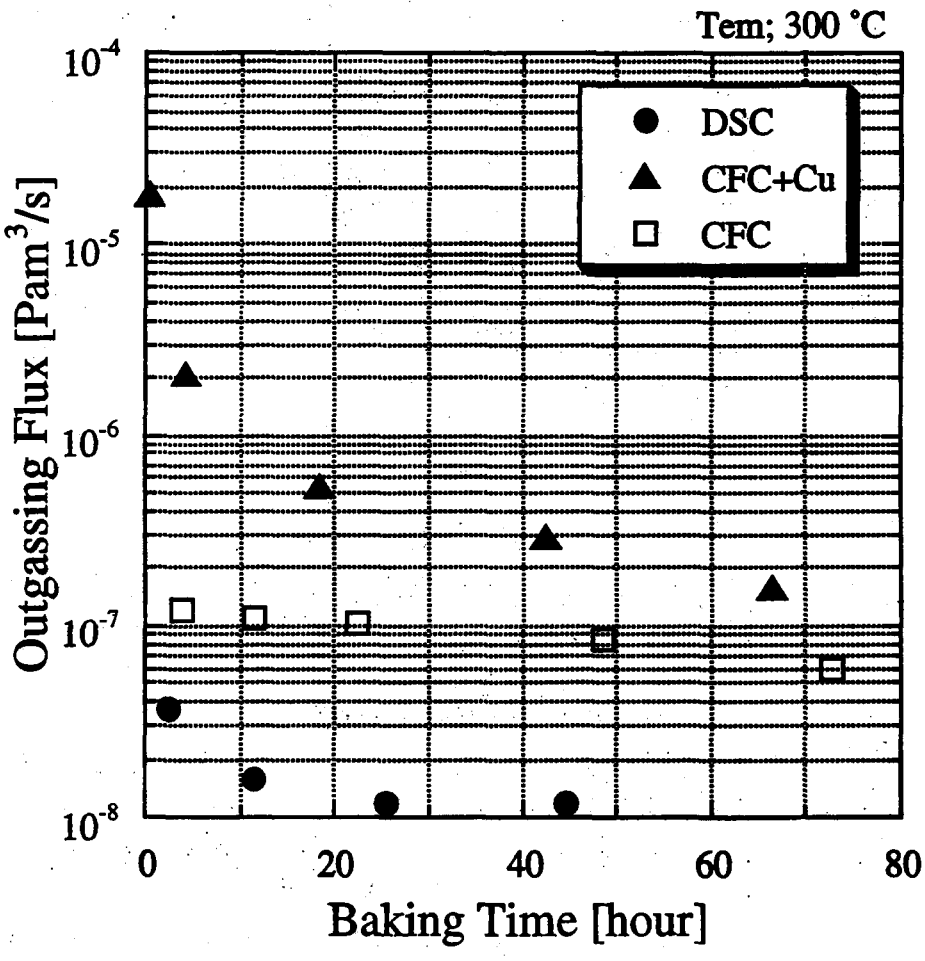

Fig.14 Outgassing flux as function of the baking treatment time.

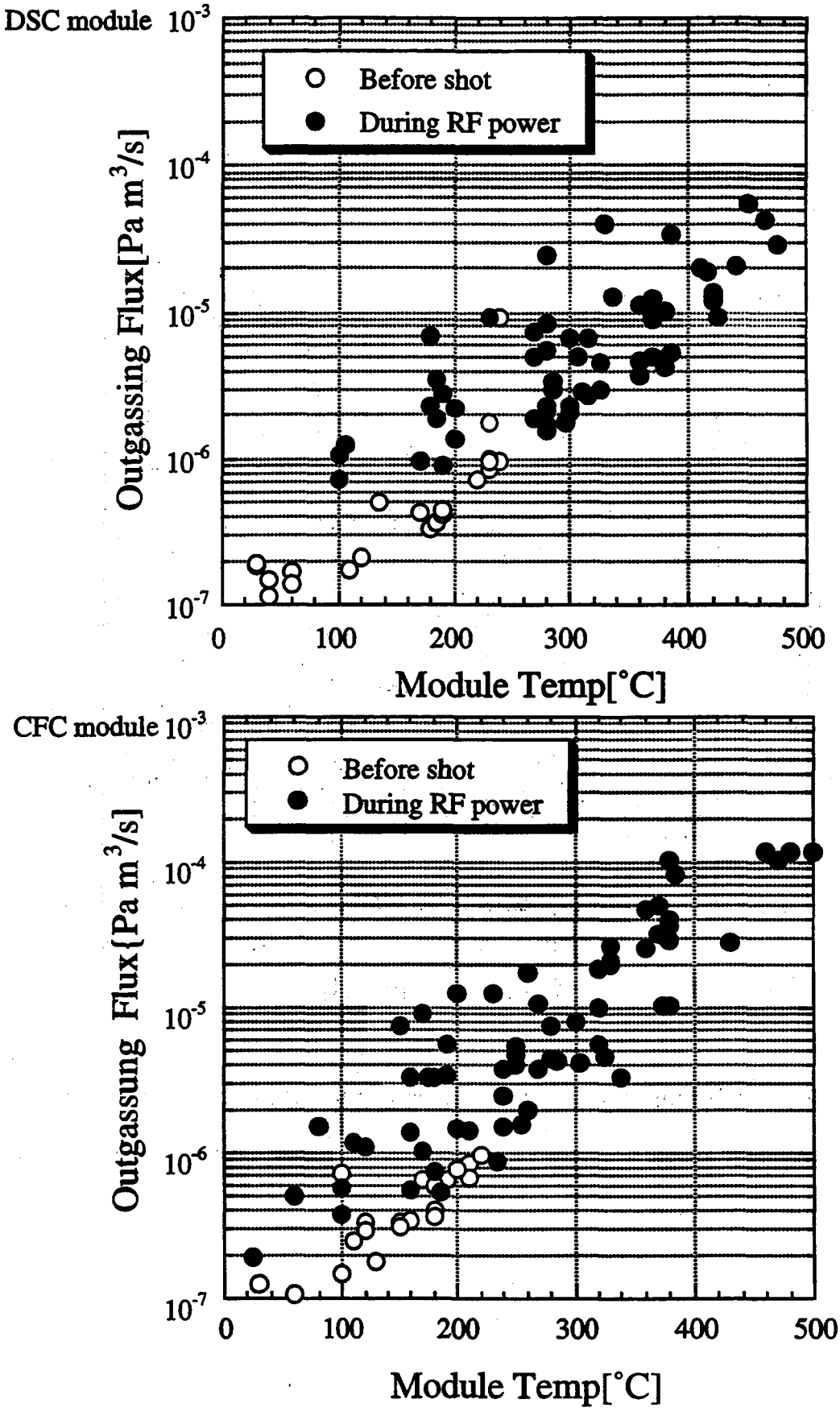

Fig.15 Outgassing flux is plotted versus the module temperature.

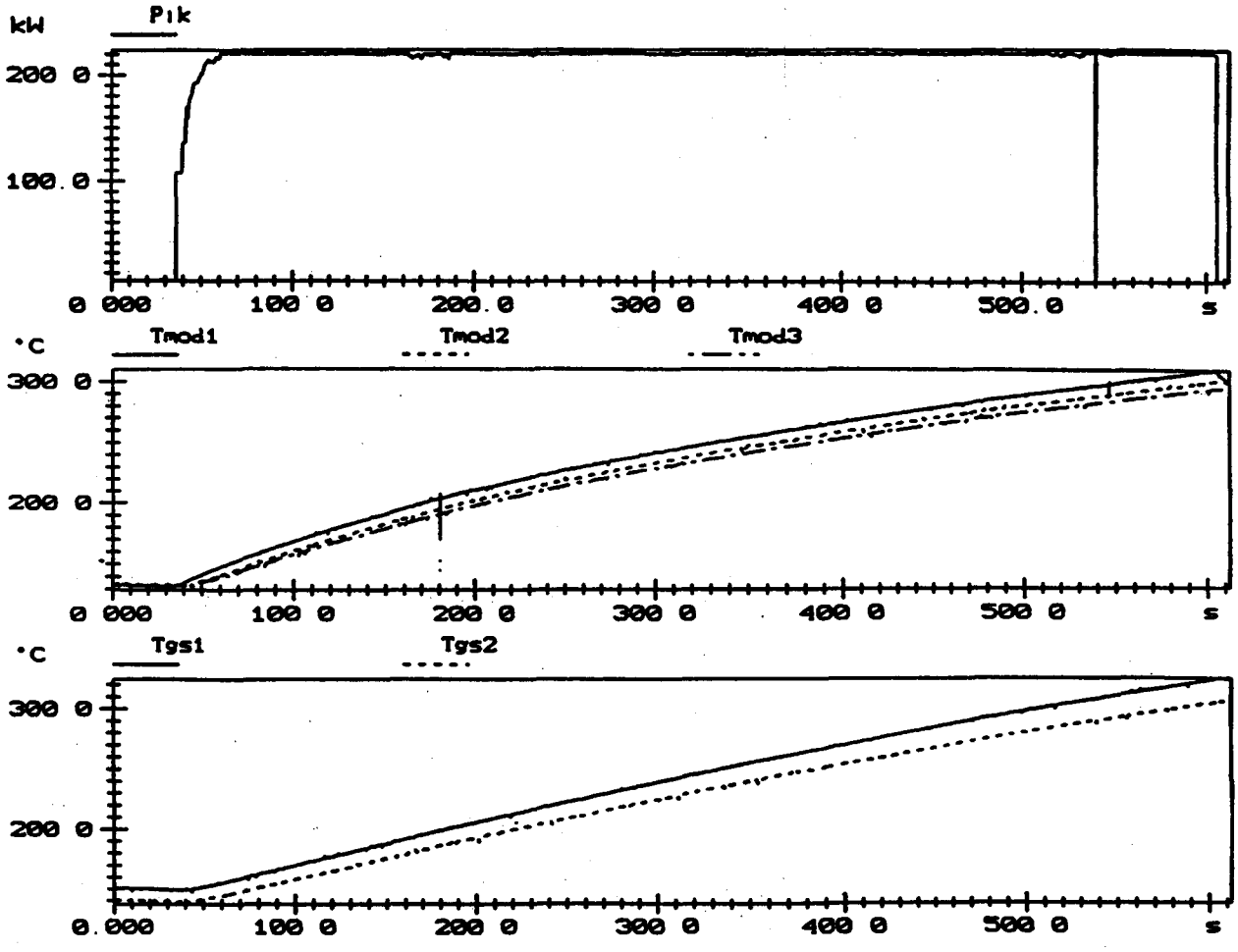

Fig.16 Time trajectory of incident RF power, DSC module temperature ($T_{module1}$, $T_{module2}$ and $T_{module3}$) and the connection waveguides (T_{gs1} and T_{gs2}).

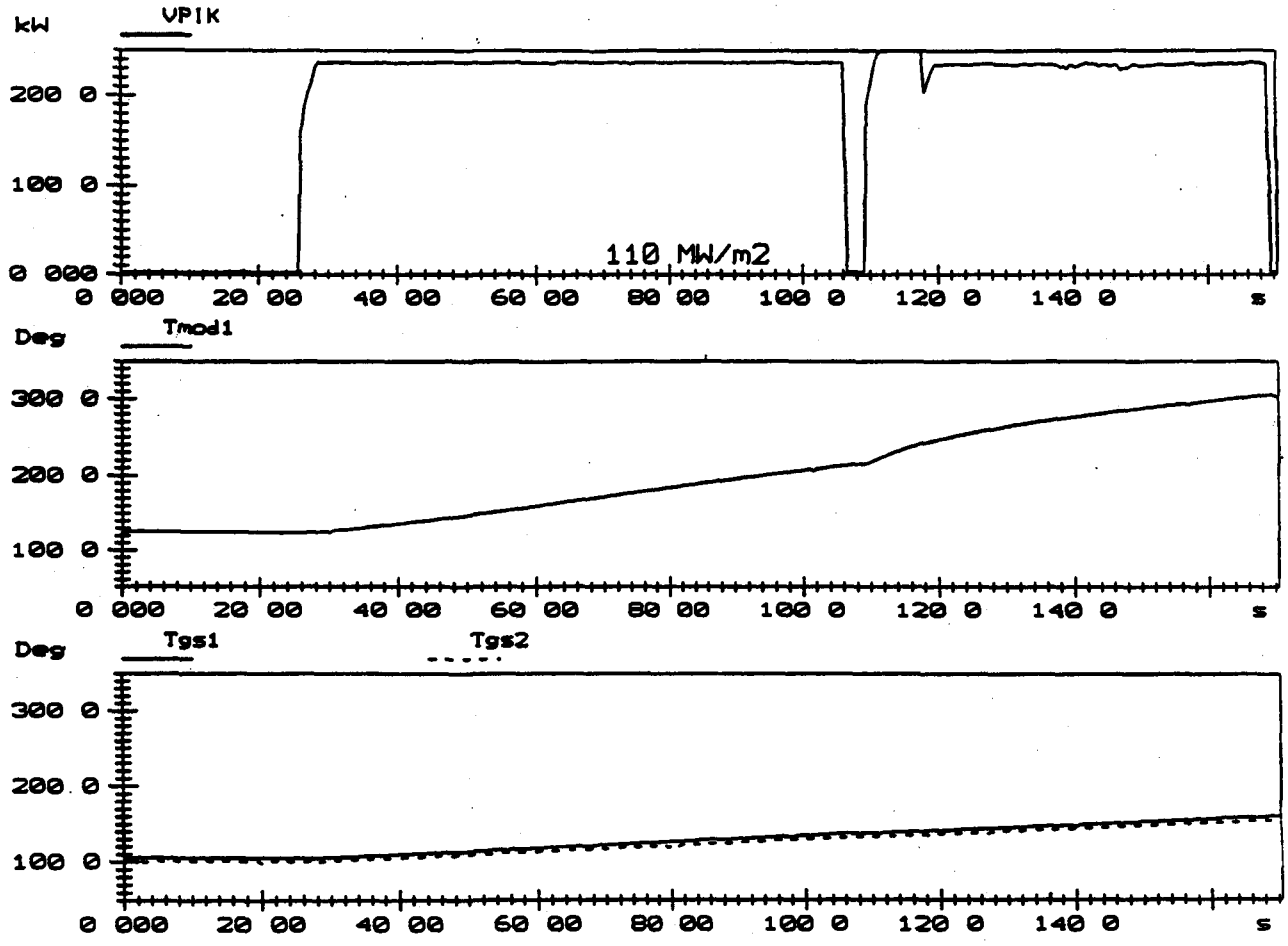

Fig.17 Time trajectory of incident RF power, CFC module temperature ($T_{module1}$) and the connection waveguides (T_{gs1} and T_{gs2}).

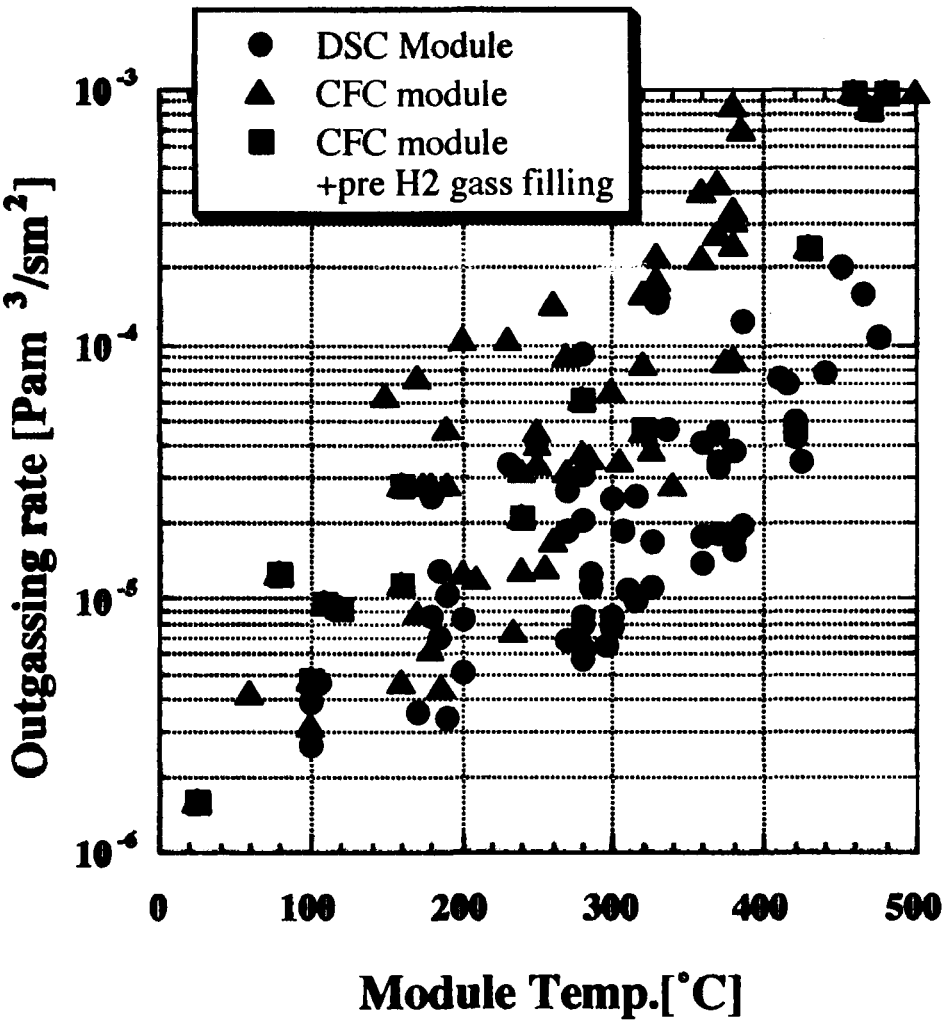

Fig.18 Outgassing rate versus the module temperature in three cases, DSC module, CFC module and CFC module with H_2 gass filling.